STATISTICAL MODELING OF ARBITRARY FLAX FIBER SHAPES FROM 2D IMAGES USING RANDOMIZED FOURIER EXPANSION

C. Mattrand*[1], A. Béakou[1], K. Charlet[1]

[1] *Clermont Université, IFMA, Institut Pascal, UMR 6602 UBP/CNRS/IFMA*
BP 10448, 63000 Clermont-Ferrand, France
* *Corresponding Author: cecile.mattrand@ifma.fr*

Keywords: flax fiber morphology, statistical modeling, Monte Carlo Simulation

Abstract

This paper focuses on modeling the scatter observed in flax fiber morphology. The proposed strategy is here based on the development of the radial distance of each 2D-fiber section to its centroid using Fourier basis functions. The Fourier coefficients as well as the maximal radial distance are considered as random variables. They are inferred from a fairly huge set of 2D optical micrographs. This methodology allows us to capture randomness in some geometrical parameters that characterize flax fiber cross-sections such as the area and perimeter.

1. Introduction

Plant fibers, which are in essence renewable, have been gaining interest over the last decade due to their appealing features. Among them, flax fibers for example exhibit competitive mechanical properties and environmentaly friendly characteristics compared with some synthetic fibers such as glass fibers [1]. Over recent years, flax fibers have therefore been gradually introduced into composite materials as a potential alternative to synthetic reinforcements. The industrial community is particularly open to these new partly green materials due to their lower carbon footprint. Nevertheless, such natural fiber composites may show a marked variability of their properties. This therefore requires large safety margins to ensure acceptable safety levels for structural components of interest, albeit undefined, thereby reducing the interest of employing natural fibers.

Scattering of derived composite behavior, *i.e.* at the macroscopic length scale, may partly result from randomness observed in flax fiber morphology and properties, *i.e.* at the microscopic length scale. Flax fiber characteristics in fact reveal significant dispersions owing to their growing harvesting and processing conditions [2, 3]. Virtual testing [4] may provide a powerful framework for studying the effect of such microstructural feature dispersions on the composite behavior variability. This subsequently may serve to control its influence on the quality and reliability of the resulting composite structures.

Micromechanical calculations have up to now mainly been developed for synthetic reinforced

composites and metal materials, see for example [5, 6, 7, 8]. From the authors' knowledge, only very few works have been devoted to the modeling of microstructures of natural fiber composites in a stochastic sense, see for example [9], even if they have specific features and might exhibit substantial scatter.

This paper proposes a first approach to modeling scatter in flax elementary fiber cross-sections that allows the simulation of virtual fibers. This contributes to the statistical description of the microstructure of composites reinforced with natural fibers, which is of prime interest for further understanding how microstructural uncertainties propagate throughout the length scales.

2. Description of the statistical modeling procedure

2.1. Strategy

The complexity of flax fiber outer geometry precludes the use of standard shape with random dimensions, such as a circle with a random radius, as shown in Figure 1. Cross-section shapes range from quasi-circles to polygons with a variable number of edges.

Figure 1. Example of five flax fiber cross-sections observed on 2D optical micrographs. The scale bar indicates 20 μm.

The random geometry of elementary flax fiber cross-sections is here modeled based on a randomized version of the truncated Fourier expansion of the radial distance of each point of a fiber boundary from its centroid. The block diagram in Figure 2 shows the basic steps of the statistical modeling procedure as well as the simulation steps of new virtual flax fibers representative of the observed ones. Some details of the strategy are given hereafter in subsection 2.2.

2.2. Details of strategy

2.2.1. Step 1: Image processing

A dozen 2D-sections of flax fibers embedded in an epoxy resin have been captured using an optical microscope. First, traces of the stem bark, other flaws and burred pixels have been manually removed from original micrographs. We also erase bundles which are not modeled in this study. Then, images have been manually processed (to make binary operation for example) so as to allow subsequent automatic extraction of fiber boundaries of one-pixel wide. The dozen observed images feature $N_e = 849$ elementary fibers. Each i^{th} elementary fiber outline forms a closed curve composed of $N^{(i)}$ pixels, $N^{(i)}$ varying from one fiber to another. An interpolation operation has first been applied to transform all coordinate vectors $\left({x_n}^{(i)}, {y_n}^{(i)}\right)_{n=0,\ldots,N^{(i)}-1}$, $\forall i = 1, \ldots, N_e$, into equal length vectors with N coordinate points. This is more suitable for subsequent statistical analyses. All coordinate vectors have then been reordered so that their starting points $\left({x_0}^{(i)}, {y_0}^{(i)}\right)$ coincide with boundary points at an angle of approximately zero.

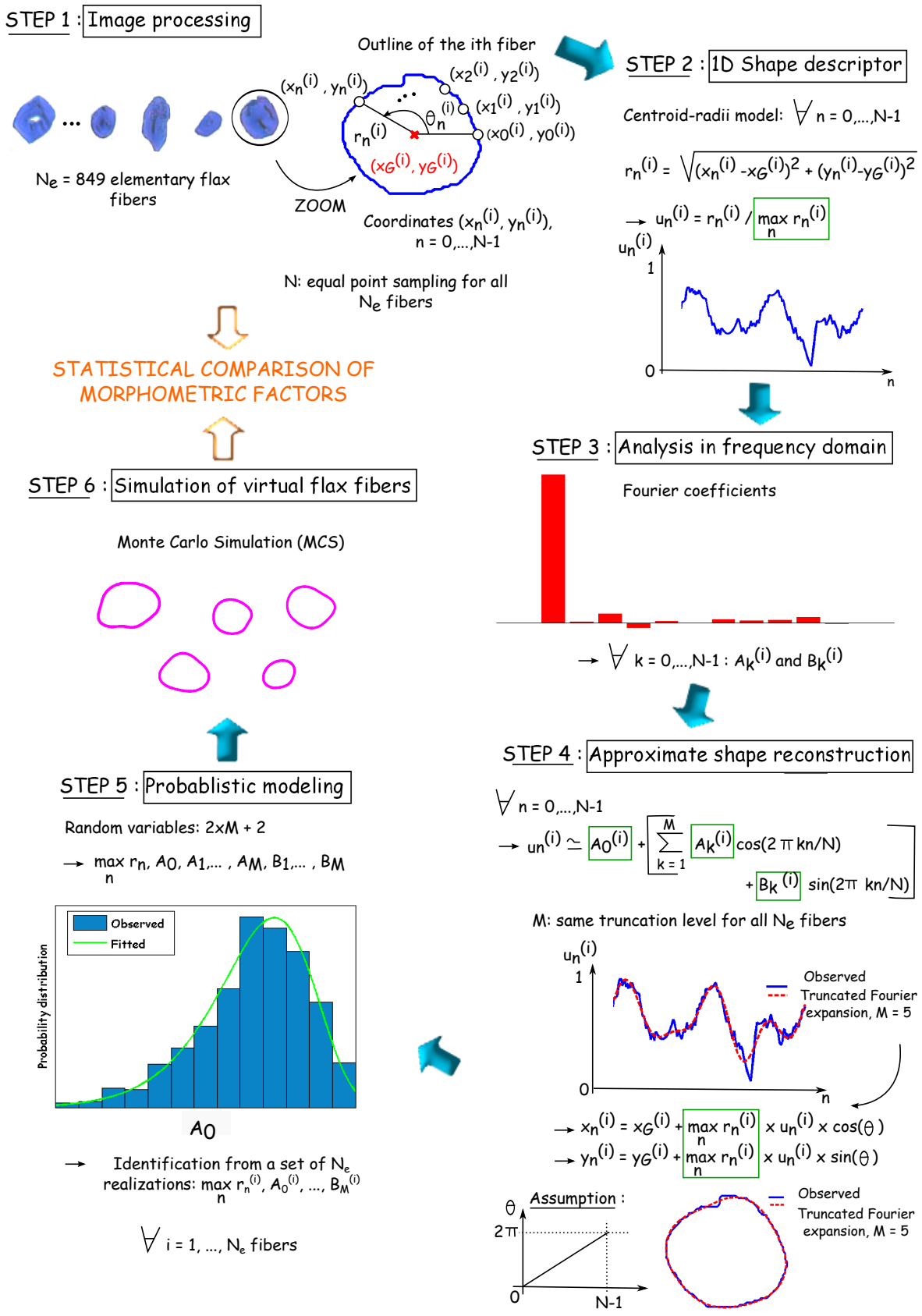

Figure 2. Block diagram of the strategy used for modeling and simulating flax fiber contours.

2.2.2. Step 2: 1D Shape descriptor

The geometry of elementary fiber cross-sections does not exhibit large concavities. We therefore consider in a first approach that 2D-boundary contours might be sufficiently well described by their radial distance from their centroid. This is one of the simplest 1D shape descriptors [10]. The centroid-radii distance function $\forall i = 1, \ldots, N_e$ and $\forall n = 0, \ldots, N-1$ is expressed by:

$$r_n{}^{(i)} = \sqrt{\left(x_n{}^{(i)} - x_G{}^{(i)}\right)^2 + \left(y_n{}^{(i)} - y_G{}^{(i)}\right)^2} = \max_n r_n{}^{(i)} \times u_n{}^{(i)} \tag{1}$$

where $\left(x_G{}^{(i)}, y_G{}^{(i)}\right)$ represents the centroid of the i^{th} shape defined by the average of the boundary coordinates and $\left(u_n{}^{(i)}\right)$ is the normalized radius vector whose values are between 0 and 1.

2.2.3. Step 3: Analysis in the frequency domain

Each i^{th} normalized centroid-radii function $\left(u_n{}^{(i)}\right)_{n=0,\ldots,N-1}$ is a discrete and periodic signal and thereby can be analyzed in the frequency domain by means of its Fourier transform. The first M-Fourier coefficients of this function for $k \in \{0, 1, \ldots, M\}$ are given by:

$$\begin{cases} A_0{}^{(i)} &= \frac{1}{N}\sum_{n=0}^{N-1} u_n{}^{(i)},\ k = 0 \\ A_k{}^{(i)} &= \frac{2}{N}\sum_{n=0}^{N-1} u_n{}^{(i)} cos(2\pi kn/N),\ 1 \le k \le M \\ B_k{}^{(i)} &= \frac{2}{N}\sum_{n=0}^{N-1} u_n{}^{(i)} sin(2\pi kn/N),\ 1 \le k \le M \end{cases} \tag{2}$$

where $M < N/2$ is a truncation level that might be applied to the Fourier expansion in order to reduce the number of variables to analyze hereafter. The reader should refer to [11] for full details of Fourier analysis.

2.2.4. Step 4: Approximate shape reconstruction

Given its first M-Fourier coefficients, each i^{th} normalized centroid-radii signal $\forall n = 0, \ldots, N-1$ may be roughly calculated by:

$$u_n{}^{(i)} \approx A_0{}^{(i)} + \sum_{k=1}^{M} A_k{}^{(i)} cos(2\pi kn/N) + B_k{}^{(i)} sin(2\pi kn/N) \tag{3}$$

which corresponds to its representation on the Fourier basis functions, that is to say, it is broken down into the cosinus and sinus functions. Then, the centroid-radii distance is obtained by:

$$r_n{}^{(i)} \approx \max_n r_n{}^{(i)} \times u_n{}^{(i)} \tag{4}$$

where $\max_n r_n^{(i)}$ is the maximum radial distance between boundary points and their centroid.

The approximate reconstruction of each i^{th} shape, *i.e.* in the original 2D-coordinate space (x, y), is finally achieved by:

$$\begin{cases} x_n^{(i)} & \approx & x_G^{(i)} + r_n^{(i)} cos(\theta) \\ y_n^{(i)} & \approx & y_G^{(i)} + r_n^{(i)} sin(\theta) \end{cases} \tag{5}$$

The current angle θ is here assumed to vary linearly between 0 and 2π with $n \in 0, \ldots, N-1$ for all N_e fibers, which is an approximation.

2.2.5. Step 5: Probabilistic modeling

The random shape of the i^{th} fiber is fully described by a coordinate vector $\left(x_n^{(i)}, y_n^{(i)}\right)_{n=0,\ldots,\ N-1}$ which should be viewed as the discretized realization of a bivariate process (X_n, Y_n), $n \in \mathbb{N}$. Since the centroid-radii function alone is used to characterize the geometry of fibers, we can replace the initial bivariate process (X_n, Y_n) by a univariate process (r_n), $n \in \mathbb{N}$. Each i^{th} realization $r_n^{(i)}$ of this process, $i = 1, \ldots, N_e$, is in turn modeled by means of a truncated Fourier expansion, see Equations 2, 3 and 4, thereby reducing the number of parameters to be analyzed. The proposed approach to model randomness in fiber shapes therefore lies in considering the coefficients of the Fourier expansion namely $A_0, A_1, \ldots, A_M, B_1, \ldots, B_M$ and the maximum radius namely $\max_n r_n$ as random variables.

The $2 \times M + 2$ random variable distributions are then fitted from a large collection of 2D images of actual flax fibers. In fact, we may recall that $N_e = 849$ elementary flax fibers have been gathered which leads to $N_e = 849$ outcomes $A_0^{(i)}, A_1^{(i)}, \ldots, A_M^{(i)}, B_1^{(i)}, \ldots, B_M^{(i)}$ and $\max_n r_n^{(i)}$ of the random variables $A_0, A_1, \ldots, A_M, B_1, \ldots, B_M$ and $\max_n r_n$. By using the Maximum Likelihood Estimation and the Kolmogorov-Smirnov test, distribution types and parameters have been identified. The maximum radial distance $\max_n r_n$ is reasonably well modeled by a truncated Gaussian distribution. A good fit is then observed between the A_0-coefficient distribution and a two parameter Weibull distribution. Finally, other A_k- and B_k-coefficients are found to be approximately normally distributed. The reader should note that the correlation coefficients between random variables are here neglected since they appear to be sufficiently low.

2.2.6. Step 6: Simulation of virtual flax fibers

Monte Carlo Simulation (MCS) is used to generate N_{sim} realizations of the above random variables. By applying the shape reconstruction procedure, see step 4 in subsection 2.2.4, N_{sim} virtual flax fiber cross-sections are then produced.

3. Results and discussion

The ability of the proposed randomized Fourier expansion model to capture the intrinsic variability observed in the morphology of flax fibers is then assessed based on simulations per-

formed in step 6, subsection 2.2.6. The statistical properties of usual morphometric factors in virtual geometries are compared with those of observed flax fibers. Five morphometric factors, namely the surface area, perimeter, Feret ratio, geodesic circularity and convexity, which feature size, elongation and tortuosity measurements, are computed for this purpose. The Feret ratio is defined by the ratio of the Feret length over the Feret width. The geodesic circularity is expressed by the ratio of the geodesic diameter over the diameter of a circular particle with the same area. Finally, the convexity is given by the ratio of the fiber area over its convex hull area, see [12] for further details on how to select relevant shape factors.

3.1. Selection of the truncation level

The influence of the truncation level M, which serves as an approximate reconstruction of the original fiber (step 4), on the fiber geometry attributes is here studied. This is based on the analysis of relative errors between morphometric factors of each observed i^{th} flax fiber cross-section and that of its approximate reconstruction, $i \in \{1, \ldots, N_e = 849\}$. We here retain the M value so that the 90%-relative errors of all shape factors are below an asymptotic value, which leads to $M = 5$ as shown in Figure 3. Then, 12 subsequent random variables are used for modeling randomness in fiber shapes.

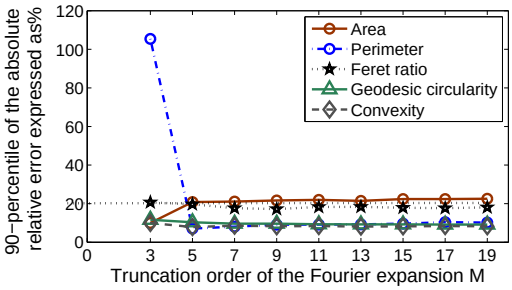

Figure 3. 90 - percentile of absolute relative error distributions (in %).

3.2. Statistical comparison of morphometric factors

Figures 4 (a) and (b) respectively plot the cumulative distributions of areas and perimeters of observed flax fiber cross-sections, that of reconstructed flax shapes with $M = 5$ and that of virtual flax fibers obtained through MCS. A very good agreement between observations and simulations is obtained. Absolute relative errors on mean values are lower than 6%, the ones on standard deviations are below 2.5%. Only the smallest percentiles of the distribution of simulated flax fiber areas are slightly overestimated compared to those of the observed flax fibers. The proposed methodology is therefore able to give a fairly good approximation of size measurements of flax fiber shapes.

Regarding the elongation (Feret ratio) and tortuosity (geodesic circularity and convexity) parameters, see figures 5, 6 (a) and (b), the mean values of simulations are generally well recovered. However, standard deviations are strongly underestimated ($< -70\%$). This might be partly explained by the choice of the 1D shape descriptor which here only models radial distance vectors therefore discarding shape information encompassed in angular vectors. By resorting to 1D shape descriptor function that encloses both x-axis and y-axis information such limitations

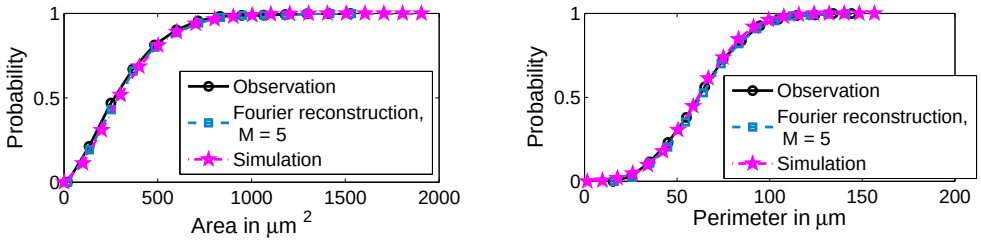

(a) Area (b) Perimeter

Figure 4. Cumulative probability plots of area and perimeter distributions for elementary flax fibers.

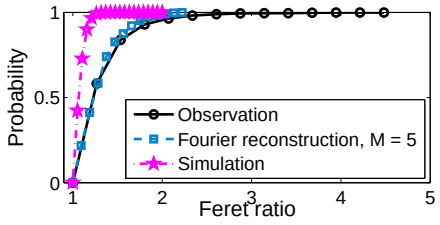

Figure 5. Cumulative probability plot of Feret ratio distributions for elementary flax fibers.

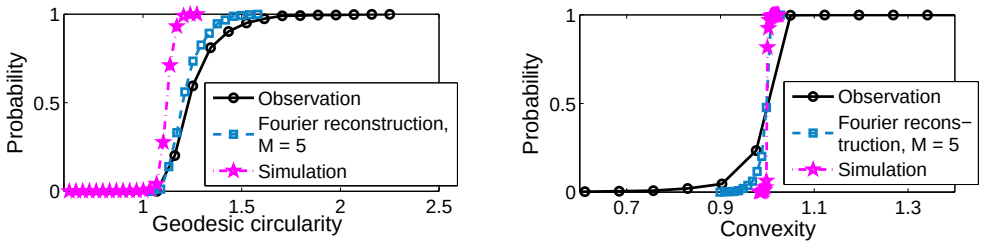

(a) Geodesic circularity (b) Convexity

Figure 6. Cumulative probability plots of geodesic circularity and convexity distributions for elementary flax fibers.

might be removed. One should replace the centroid-radii model by the complex coordinate function within the strategy for example. The authors have performed such work in [13]. The randomized Fourier expansion of the complex coordinate function is found to be relevant to capture randomness in both size, elongation and tortuosity parameters of flax fiber shapes.

4. Conclusion

Plant fibers are directly sourced from nature and therefore suffer from inherent variability. This may cause substantial dispersions of their derived composite properties which should therefore be mastered so that natural fibers become more attractive for structural applications. This paper proposes a procedure to model dispersions in the geometry of 2D flax fiber cross-sections. This methodology is hoped to enable the simulation of virtual flax fiber shapes which are statistically representative of the observed ones. Results show that virtual fibers have the same statistics as those of observed fibers regarding the area and perimeter parameters. However, elongation and tortuosity measurements are not rendered accurately enough by the method presented here. The authors propose improvements for the proposed methodology in [13], which allows us to obtain

a better match between observations and simulations for all morphometric parameters.

This work should be viewed as an essential step towards the numerical modeling of plant fiber reinforced composites with the aim of gaining insights into the influence of microstructural uncertainties on the macroscopic properties of the resulting composites.

References

[1] L. Yan, N. Chouw, and K. Jayaraman. Flax fibre and its composites A review. *Composites: Part B*, 56:296–317, 2014.

[2] K. Charlet, J.-P. Jernot, J. Breard, and M. Gomina. Scattering of morphological and mechanical properties of flax fibres. *Industrial Crops and Products*, 32:220–224, 2010.

[3] J.L. Thomason, J. Carruthers, J. Kelly, and G. Johnson. Fibre cross-section determination and variability in sisal and flax and its effects on fibre performance characterisation. *Composites Science and Technology*, 71:1008–1015, 2011.

[4] M.I. Okereke, A.I. Akpoyomare, and M.S. Bingley. Virtual testing of advanced composites, cellular materials and biomaterials: a review. *Composites: Part B*, 60:637–662, 2014.

[5] Z. Shan and A.M. Gokhale. Digital image analysis and microstructure modeling tools for microstructure sensitive design of materials. *International Journal of Plasticity*, 20:1347–1370, 2004.

[6] H. Singh, A.M. Gokhale, Y. Mao, and J.E. Spowart. Computer simulations of realistic microstructures of discontinuously reinforced aluminum alloy (DRA) composites. *Acta Materialia*, 54:2131–2143, 2006.

[7] D. Trias, J. Costa, J.A. Mayugo, and J.E. Hurtado. Random models versus periodic models for fibre reinforced composites. *Computational Materials Science*, 38:316–324, 2006.

[8] V. Romanov, S.V. Lomov, Y. Swolfs, S. Orlova, Gorbatikh L., and Verpoest I. Statistical analysis of real and simulated fibre arrangements in unidirectional composites. *Composites Science and Technology*, 87:126–134, 2013.

[9] M. Faessel, C. Delisée, F. Bos, and P. Castéra. 3D Modelling of random cellulosic fibrous networks based on x-ray tomography and image analysis. *Composites Science and Technology*, 65:1931–1940, 2005.

[10] D. Zhang and G. Lu. A Comparative Study of Fourier Descriptors for Shape Representation and Retrieval. In *ACCV2002: The 5th Asian Conference on Computer Vision, 2325 January 2002, Melbourne, Australia*, 2002.

[11] S.W. Smith. *The Scientist and Engineer's Guide to Digital Signal Processing*. 1998.

[12] D. Legland and J. Beaugrand. Automated clustering of lignocellulosic fibres based on morphometric features and using clustering of variables. *Industrial Crops and Products*, 45:253–261, 2013.

[13] C. Mattrand, A. Béakou, and K. Charlet. Numerical modeling of the flax fiber morphology variability. *submitted to Composites: Part A*, 2014.